Biochem J. (1989) 262, 439–447 (Printed in Great Britain)

Effects on ATPase activity of monoclonal antibodies raised against ($Ca^{2+}+Mg^{2+}$)-ATPase from rabbit skeletal muscle sarcoplasmic reticulum and their correlation with epitope location

John COLYER,* Ana M. MATA,† Anthony G. LEE and J. Malcolm EAST
Department of Biochemistry, University of Southampton, Southampton SO9 3TU, U.K.

A total of 28 monoclonal antibodies have been raised against the ($Ca^{2+}+Mg^{2+}$)-ATPase of rabbit skeletal muscle sarcoplasmic reticulum. Epitope mapping, using protein fragments generated by proteolysis, indicates that these antibodies include examples binding to at least four distinct epitopes on the A_1 and B tryptic fragments of the ATPase. Competition data also show that the 28 antibodies are directed against at least five spatially distinct regions. Altogether, nine inhibitory antibodies were produced: six of these inhibitory antibodies mapped to the same spatial region, although they appear to bind to two distinct epitopes located within the hinge region and the nucleotide-binding domains of current structural models; one antibody bound to an epitope located within the phosphorylation domain and the stalk-transmembranous region designated M_4S_4 by Brandl, Green, Korczak & MacLennan [(1986) Cell **44**, 597–607]. Two of the inhibitory antibodies recognized assembled epitopes exclusively and could not be mapped. Binding to four of the five identified spatial regions was without effect on activity. These data show that the inhibition of catalytic activity by monoclonal antibodies is achieved only by binding to defined regions of the ATPase and they may therefore provide useful probes of structure–function relationships.

INTRODUCTION

The ($Ca^{2+}+Mg^{2+}$)-ATPase of sarcoplasmic reticulum (SR) is the calcium pump responsible for translocating calcium from the sarcoplasm into the SR. This pump belongs, along with the ($Na^+ + K^+$)-ATPase, to a class of cation-transport ATPases which show sequence similarity and are believed to share a similar transport mechanism (Brandl *et al.*, 1986). The proposed mechanism involves switching of the protein between two conformational states, designated E1 and E2. In this model it is the phosphorylation by ATP of the E1 form to E1-*P* and its subsequent conversion to E2-*P* which constitutes the transport step (de Meis & Vianna, 1979; MacLennan *et al.*, 1985; Gould *et al.*, 1986). Structural models have been proposed for these ATPases on the basis of sequence data. The models propose that these transport protein are organized into functional domains, with discrete domains for nucleotide and calcium binding and a transduction domain responsible for transmitting conformational changes between domains coupling ATP hydrolysis to calcium translocation (MacLennan *et al.*, 1985; Shull *et al.*, 1985). To gain further information about structure–function relationships, a number of laboratories have produced monoclonal antibodies (mAbs) directed against these ATPases. Ball *et al.* (1986) obtained a mAb against the ($Na^+ + K^+$)-ATPase which modifies an ATP-induced conformation change and also inhibits phosphorylation of the ATPase following ATP binding. Similarly Schenk *et al.* (1984) were able to demonstrate the effect of a mAb on the sodium-dependent phosphorylation of this protein. The production of inhibitory mAbs against the ($Ca^{2+}+Mg^{2+}$)-ATPase has been less successful. Although a number of mAbs against ($Ca^{2+}+Mg^{2+}$)-ATPase have been produced (Zubrzycka-Gaarn *et al.*, 1984; Levitsky *et al.*, 1987; Dulhunty *et al.*, 1987) only three were inhibitory.

We have produced 28 mAbs against the ($Ca^{2+}+Mg^{2+}$)-ATPase which have been characterized by epitope mapping and by their ability to compete with each other for binding to the ATPase. These data have been correlated with the effects of mAbs on the steady-state ATPase activity of the ($Ca^{2+}+Mg^{2+}$)-ATPase in order to evaluate the use of mAbs in defining the involvement of particular domains in ATPase function.

MATERIALS AND METHODS

($Ca^{2+}+Mg^{2+}$)-ATPase was prepared from female rabbit (New Zealand White) hind-leg and back muscle as described by Froud & Lee (1986).

A total of 28 mAbs were generated by intraperitoneal immunizations of female BALB/c mice with 100 μg of ($Ca^{2+}+Mg^{2+}$)-ATPase in Freund's complete adjuvant (FCA) (three fusions were performed in this manner and the mAbs were designated 1/, A/ and B/) or with 500 μg of SR (mAbs designated Y/). After 3–4 weeks the mice were boosted by an intravenous injection of 100 μg of ATPase or 100 μg of ATPase-depleted SR [produced by the partial removal of the ATPase on an affinity column (see below for details)] as appropriate. (The purpose of using ATPase-depleted SR was to stimulate the pro-

Abbreviations used: SR, sarcoplasmic reticulum; BSA, bovine serum albumin; FCA, Freund's complete adjuvant; FITC, fluorescein isothiocyanate; mAb, monoclonal antibody; PBS, phosphate-buffered saline; KLH, keyhole-limpet haemocyanin; MGA, Met-Glu-Ala-Ala-His-Ser-Thr-Glu-Glu-Cys; CKF, Cys-Lys-Phe-Ile-Ala-Arg-Asn-Tyr-Leu-Glu-Gly.

* Present address: Department of Biochemistry, University of Calgary, 3330 Hospital Drive NW, Calgary T2N 4N1, Alberta, Canada.
† Present address: Universidad de Extremadura, Departamento de Bioquímica Y Biología Molecular Y Genética, Badajoz 06080, Spain.

duction of antibodies against SR components other than the ATPase, but in fact this produced only hybrids secreting anti-ATPase mAbs.) The spleens of these mice were removed 3 days later and the spleen cells fused with P3/NS 1/1-Ag4-1 myeloma cells at a ratio of 3:1 in 50% poly(ethylene glycol) 4000 (Merck) as described by Galfrè & Milstein (1981). Hybridoma cells were maintained on macrophage feeder layers on selective medium, and anti-ATPase antibodies were identified by e.l.i.s.a. (Hudson & Hay, 1983) after 10 days, using e.l.i.s.a. plates coated with either 1 μg of ATPase or 5 μg of SR per well. Culture medium (100 μl) from rapidly growing cells was added to the plates with 100 μl of phosphate-buffered saline (PBS; 137 mM-NaCl/2.7 mM-KCl/8.1 mM-Na_2HPO_4/1.5 mM-KH_2PO_4, pH 7.2) containing 0.05% Tween-20, pH 7.2 (PBS/Tween). Positive hybridoma cell lines were cloned twice by limiting dilution. Antibodies for use in the following experiments were purified from ascites fluid. Isotyping of mAbs was performed by e.l.i.s.a. using isotype-specific antibodies. MAbs of class IgG_1, IgG_{2a} and IgG_{2b} were purified from ascites fluid on a Protein A–Sepharose column (Ey *et al.*, 1978). IgM mAbs were purified on hydroxyapatite columns by the method of Stanker *et al.* (1985). Partially purified antibodies were prepared by precipitation with 40% saturated ammonium sulphate.

For immunoblotting, proteins (100 μg per gel) were separated on 10% polyacrylamide gels (Laemmli, 1970) and transferred electrophoretically to nitrocellulose paper (0.45 μm, Schleicher and Schuell) as described by Towbin *et al.* (1977). A strip of nitrocellulose was incubated overnight at 4 °C in PBS containing 0.3% Tween-20 and gold-stained according to the method of Moeremans *et al.* (1985) with a 15 nm gold sol in 10 mM-citrate/phosphate buffer, pH 5.0. The remaining nitrocellulose was blocked with 5% low-fat dried milk in PBS, cut into strips and exposed sequentially in PBS/Tween to mAb (1–5 $\mu g \cdot ml^{-1}$, 1 h) or anti-peptide antibodies (1:50 dilution, 1 h), horse-radish peroxidase conjugated to sheep anti-(mouse IgG,A,M) (Sera-Tec, diluted 1:5000) and substrate (Biorad, 4-chloro-1-naphthol plus 0.15% H_2O_2), washing with PBS/Tween between steps.

A modified e.l.i.s.a. technique was employed to determined the preference of mAb binding to native or heat-denatured ($Ca^{2+} + Mg^{2+}$)-ATPase. Monoclonal antibody (0.7 μg) was incubated overnight at 4 °C in PBS/Tween with the ATPase (2–160 $\mu g \cdot ml^{-1}$) in either the native form or after heat denaturation (100 °C, 3 min). The incubation mixture was transferred to e.l.i.s.a. plates coated with ATPase and the e.l.i.s.a. was performed as outlined above.

For competition binding studies, labelled antibodies were produced by culturing approx. 10^6 hybridoma cells for 6–8 h in 1 ml of methionine-free Eagle's Medium with Earle's salts (Gibco) supplemented with 10% foetal calf serum and 30 μCi of [^{35}S]methionine (Amersham International). Poly(vinyl chloride) e.l.i.s.a. plates coated with ($Ca^{2+} + Mg^{2+}$)-ATPase (1 μg per well) were incubated for 3 h with 10 μg of purified antibody or an equivalent amount of antibody partially purified by ammonium sulphate precipitation. Aliquots (10–20 μl) of radiolabelled mAbs were added to the wells and the incubation continued for a further 1 h. Bound antibody was determination by liquid scintillation counting of individual wells cut from e.l.i.s.a. plates in 4 ml of Labscint (Lablogic).

Trypsin digestion of ATPase was performed as described in Garcia de Ancos & Inesi (1988). ATPase (250 μg) was digested with 12.5 μg of trypsin (type 1, Sigma) for 30 min in 0.1 ml of 20 mM-Mops/800 mM-KCl, pH 6.8. The reaction was terminated by adding soya bean trypsin inhibitor (Sigma) (inhibitor/trypsin of 2:1 molar ratio) followed by solubilization in Laemmli (1970) sample buffer containing 2% SDS and 10% β-mercaptoethanol. About 80 μg of the digest was loaded on to 12% polyacrylamide gels and the fragments electrophoretically separated (20 mA, 2 h) by the method of Laemmli (1970). Proteins were transferred to nitrocellulose paper and probed with mAbs and anti-peptide antibodies as outlined above. Some antibodies were mapped to only the major proteolytic fragments A and B (Thorley-Lawson & Green, 1973), in which case 250 μg of ATPase was digested with 0.3 μg of trypsin for 60 min and the digest treated as above. Fluorescein isothiocyanate (FITC)-labelled ATPase was used in these studies so that anti-fluorescein antibodies could be used to locate fragments containing fluorescein. The ATPase was labelled with FITC at a molar ratio of FITC/ATPase of 1:2 in buffer (0.25 M-sucrose/1 M-KCl/50 mM-potassium phosphate, pH 8.0) as described in Froud & Lee (1986).

V8 protease digestion was carried out as outlined by Cleveland *et al.* (1977). FITC-labelled ATPase was digested with 12.5 μg of *Staphylococcus aureus* V8 protease (EC 3.4.21.19, Sigma, type XVII) in 0.125 M-Tris/HCl, pH 6.8, containing 10% glycerol, 0.5% SDS and 0.001% Bromophenol Blue. The digestion was terminated after 5 min by the addition of SDS (final concentration 2%) and β-mercaptoethanol (final concentration 10%) followed by boiling for 2 min. Gels (12.5%) were loaded with 110 μg of digested ATPase and electrophoresed for about 2 h at 20 mA. Proteins were transferred and probed as outlined above.

ATPase activity was determined following a 60 min pre-incubation of 100 μg of ATPase with affinity-purified antibody (3:1 mAb/ATPase by weight) in 120 μl of Hepes/KOH, pH 7.2, or for 2 h with mAbs purified by ammonium sulphate precipitation. In the latter case the mAb/ATPase ratio was estimated to be 4:1 based on scans of polyacrylamide gels of the mAbs purified by precipitation. In some assays the pre-incubation and the assay itself were carried out in the presence of the detergent $C_{12}E_8$ (0.5 mM) (Calbiochem). The ATPase activity of the ($Ca^{2+} + Mg^{2+}$)-ATPase was determined at 25 °C using a coupled enzyme assay (East & Lee, 1982).

ATPase-depleted SR was prepared by solubilizing 3.4 mg of SR in 1.6 ml of PBS (brought to pH 8.0 with KOH) containing potassium deoxycholate (1.9 $mg \cdot ml^{-1}$; PBS/DOC). The solubilized SR was passed through a 3 ml Protein A column containing bound mAb 4^c (8 mg). The eluate was collected from the column and was shown by SDS/polyacrylamide-gel electrophoresis to contain only 30% ATPase compared with the 80% in SR.

Peptides Met-Glu-Ala-Ala-His-Ser-Thr-Glu-Glu-Cys (MGA) and Cys-Lys-Phe-Ile-Ala-Arg-Asn-Tyr-Leu-Glu-Gly (CKF) were synthesized by the methods of Sheppard (Atherton *et al.*, 1981) and Merrifield (1986) respectively. These two sequences correspond to the *N*- and *C*-terminal segments of the ($Ca^{2+} + Mg^{2+}$)-ATPase (Brandl *et al.*, 1986) but include an extra cysteine residue for coupling to the carrier. The peptides were coupled to keyhole-limpet haemocyanin (KLH) by the protocol of

Table 1. Immunization protocols for the production of mAbs against (Ca^{2+} + Mg^{2+})-ATPase, characterization of mAb isotypes and recognition of the ATPase on Western blots

Antibodies were isotyped by e.l.i.s.a. using isotype-specific antibodies. (Ca^{2+} + Mg^{2+})-ATPase separated on polyacrylamide gels was probed by Western blotting using monoclonal antibodies which recognized the ATPase in e.l.i.s.a. Antibodies have been coded according to the information available concerning the location of their epitopes. MAbs designated 'U' did not recognize the ATPase on Western blots and their epitopes could not be mapped by the approach used here; the epitopes of those designated 'B' have only been mapped to the B tryptic fragment, whereas the epitopes of mAbs designated '1–4' have been mapped more extensively to particular segments of the ATPase (see Fig. 5 for details of epitope locations).

Immunization protocol	mAb	Antibody class	Recognition of ATPase on Western blots	mAb designation on the basis of epitope mapping
Fusion 1: 100 μg of ATPase in FCA (day 1); boost of 100 μg of ATPase (day 30)	1/2H7	IgG_1	Yes	4^a
	1/3D2	IgG_1	No	U^a
Fusion A: protocol as above	A/1H8	IgM	No	U^b
	A/2D3	IgM	Yes	1^a
	A/4H3	IgG_1	Yes	4^b
Fusion B: protocol as above	B/3D6	IgG_{2b}	Weakly	4^c
	B/4A10	IgG_1	Yes	B^a
	B/4E10	IgM	No	U^c
	B/4H3	IgG_1	Yes	4^d
Fusion Y: 500 μg of SR in FCA (day 1); boost of 100 μg of ATPase-depleted SR (day 34)	Y/1B11	IgG_1	Yes	B^b
	Y/1D9	IgG_{2b}	Yes	B^c
	Y/1F4	IgG_{2b}	Yes	3^a
	Y/1G4	IgG_1	Yes	B^d
	Y/1G6	IgG_{2a}	Yes	B^e
	Y/1H12	IgG_{2b}	Yes	2^a
	Y/2A2	IgG_{2a}	Yes	2^b
	Y/2D11	IgG_1	Yes	B^f
	Y/2D8	IgG_1	Yes	3^b
	Y/2D12	IgM	Weakly	U^d
	Y/2E9	IgG_1	Yes	3^a
	Y/3B3	IgM	Yes	B^g
	Y/3G6	IgG_1	Yes	3^d
	Y/3C8	IgG_{2b}	Yes	3^e
	Y/3H2	IgG_{2a}	Yes	B^h
	Y/3H5	IgG_1	Yes	2^a
	Y/4A2	IgG_1	Yes	B^i
	Y/4A11	IgG_{2b}	Yes	B^j
	Y/4D6	IgG_1	Yes	2^d

Green *et al.* (1982). New Zealand White rabbits were immunized subcutaneously with 500 μg of KLH–peptide in FCA and boosted by intramuscular injection 40 days later with 250 μg of KLH–peptide in FCA. Blood was collected 7–14 days later, and the serum was separated and stored at −70 °C. Anti-fluorescein antiserum was prepared using the above immunization schedule with FITC coupled to bovine serum albumin (FITC–BSA). FITC–BSA was prepared by incubating 10 mg of BSA with 5 mg of FITC in 1 ml of 1 M-$NaHCO_3$ for 1 h. The conjugate was separated from unreacted FITC on a Sephadex G-50 column, dialysed overnight against PBS and 400 μg of the conjugate in FCA was used in the immunization protocol.

RESULTS

Altogether, 28 mAbs were produced in this study. Table 1 shows that 67% of the mAbs produced using ATPase as an immunogen were IgGs, whereas mAbs produced using ATPase-depleted SR were 85% IgGs. All of the mAbs from the Y-fusion recognized the ATPase in Western blotting, but only about 60% of the mAbs from the other fusions were able to do this (see Fig. 1 and Table 1).

To simplify the discussion of results, the mAbs catalogued in Table 1 have been coded according to the mapping of their epitopes. Mabs designated 'U' could not be mapped by the approach used here; those designated 'B' were mapped to the B tryptic-digest fragment but were not characterized further, and mAbs designated '1–4' have been mapped to particular segments of the ATPase (see Fig. 5 for summary).

Three mAbs (U^{a-c}) were unable to recognize the ATPase in Western blots (Fig. 1, Table 1). To test whether these mAbs could bind to the native ATPase, competitive binding experiments were carried out. MAbs U^{a-c} were incubated overnight with native or heat-denatured ATPase to estimate the amount of unbound antibody in the incubate. Fig. 2(*a*) shows that mAb U^a, which does not bind to the ATPase after Western blotting (Fig. 1), is depleted only after incubation with native ATPase, as were mAbs U^b and U^c (results not shown), indicating that they cannot bind to denatured ATPase

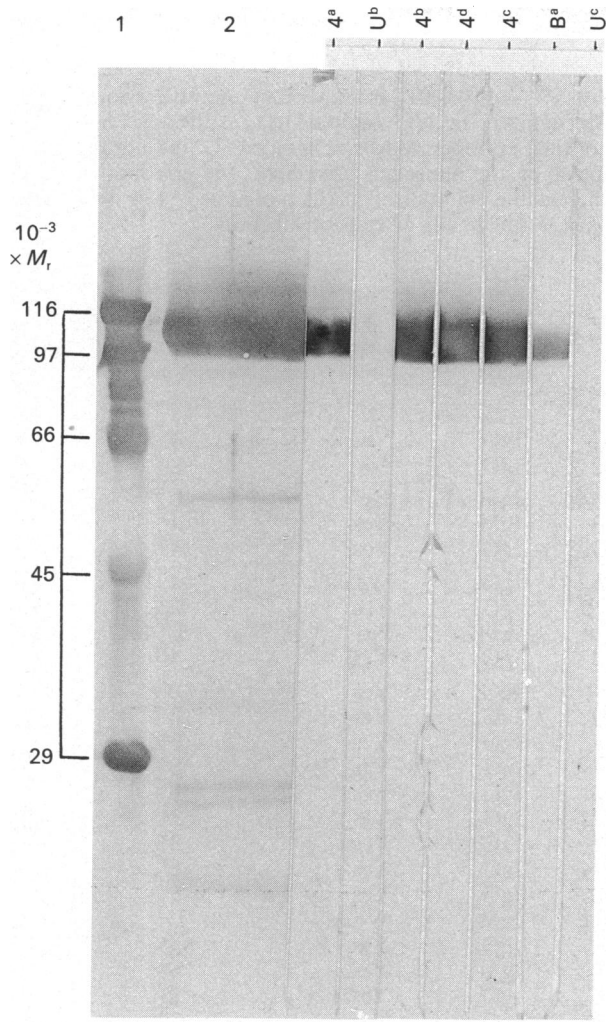

Fig. 1. Recognition of $(Ca^{2+}+Mg^{2+})$-ATPase on Western blots by monoclonal antibodies

ATPase (100 μg) was electrophoresed on a 10% polyacrylamide gel (a small well was provided for M_r standards). The proteins were transferred to nitrocellulose and a strip containing the M_r standards and a section of the ATPase lane was stained for protein with colloidal gold (lanes 1 and 2 respectively). The remaining nitrocellulose was cut into strips, incubated overnight with a blocking agent and incubated sequentially with monoclonal antibodies (as designated), horseradish-peroxidase-conjugated second antibody, and peroxidase substrate.

and therefore presumably bind to assembled epitopes. Fig 2(*b*) shows that mAb 4^c, which is able to bind to the ATPase in Western blots, cannot discriminate between the native and denatured forms of the ATPase, whereas mAb 4^a (Fig. 2*c*) showed a slight preference for the denatured form of the ATPase as did mAbs 4^b and 4^d (results not shown). This suggests that these three mAbs bind to an epitope which is partly occluded in the native ATPase.

Epitope mapping by limited proteolysis and Western blotting was performed for most of the mAbs which recognized the ATPase on Western blots. In initial studies this involved locating the epitopes on either the A or B tryptic fragments of the ATPase (Thorley-Lawson & Green, 1973; see also Fig. 5) (data summarized in Table 1). The detailed analysis of epitope location involved locating on Western blots the proteolysis products still containing either the *N*-terminus of the ATPase (identified by anti-peptide antibodies against *N*-terminal residues; lanes labelled MGA in Figs. 3*a* and 3*b*) or the *C*-terminus (identified by anti-peptide antibodies against *C*-terminal residues, tracks labelled CKF in Figs. 3*a* and 3*b*). By identifying which of these terminal fragments binds a particular mAb it is possible to identify the protein segment on which the epitope is located (see also Figs. 4*a* and 4*b*). Taking mAb 4^a as an example and comparing its binding profile in Fig. 3(*a*) with that of the anti-*C*-terminal antibodies (lane CKF) it can be seen that both the mAb and the anti-peptide antibodies recognize the ATPase with an M_r of around 110000. A series of bands in lane CKF including a broad band with an M_r of about 45000 (according to the M_r standards in lane 1) are all recognized by mAb 4^a. None of the smaller M_r fragments recognized by the anti-*C*-terminal antibodies were recognized by mAb 4^a, indicating that the epitope had been removed by proteolytic cleavage at the next proteolytic site, proximal to the *C*-terminus. Therefore, the epitope for mAb 4^a is located in the region corresponding to the difference between the smallest *C*-terminal-containing fragment recognized by mAb 4^a and the largest *C*-terminal-containing fragment which is not recognized. This information is presented in diagramatic form in Fig 4(*a*) and is summarized in Fig. 5.

It cannot be ruled out in such studies that certain of the bands seen on the Western blot contain more than one polypeptide, which could give rise to errors in assigning identities to these bands. However, since the mapping was performed with two proteases and the results from both studies are in close agreement (Fig. 5), it seems unlikely that fragments have been incorrectly identified.

The accuracy of the above technique is limited by the M_r determinations of the *N*- and *C*-terminal-containing fragments identified with the anti-peptide antibodies. M_r values have been assigned to fragments using the accurately known M_r values of the ATPase (109000) and of the first tryptic digestion products A (55400) and B (53800) and of the secondary tryptic fragments of A, A_1 (33200) and A_2 (22100) (Thorley-Lawson & Green, 1973). As shown in Fig. 3(*a*) (lane 2), tryptic digestion of FITC–ATPase gave a band by gold staining at an M_r of about 50000 according to the nearest molecular mass marker protein at M_r-45000. That this digest product is the A fragment of M_r-55400 (MacLennan *et al.*, 1985) is confirmed both by its recognition by the anti-*N*-terminal antibody (Fig. 3*a*, lane MGA) and its failure to be recognized by an anti-fluorescein antibody (Fig. 3*a*, lane FITC–BSA), since the FITC labels Lys-514 on the B tryptic fragment. The B fragment is not clear on the gels, but the A_2 tryptic fragment detected at M_r-22000 as expected is detected by the anti-*N*-terminal antibody (Fig. 3*a*, lane MGA) although it was not visible on the gold-stained lane (Fig. 3*a*, lane 2). In fact when the combined M_r data from the M_r markers and the identified tryptic digest fragments (A and A_2) were plotted (i.e. log M_r against relative retention) only the M_r marker for 45000 was significantly off the straight line. The combined data have been used in assigning all apparent M_r values which follow. In addition to the A fragment a 31000-M_r fragment is also revealed by gold staining. This band

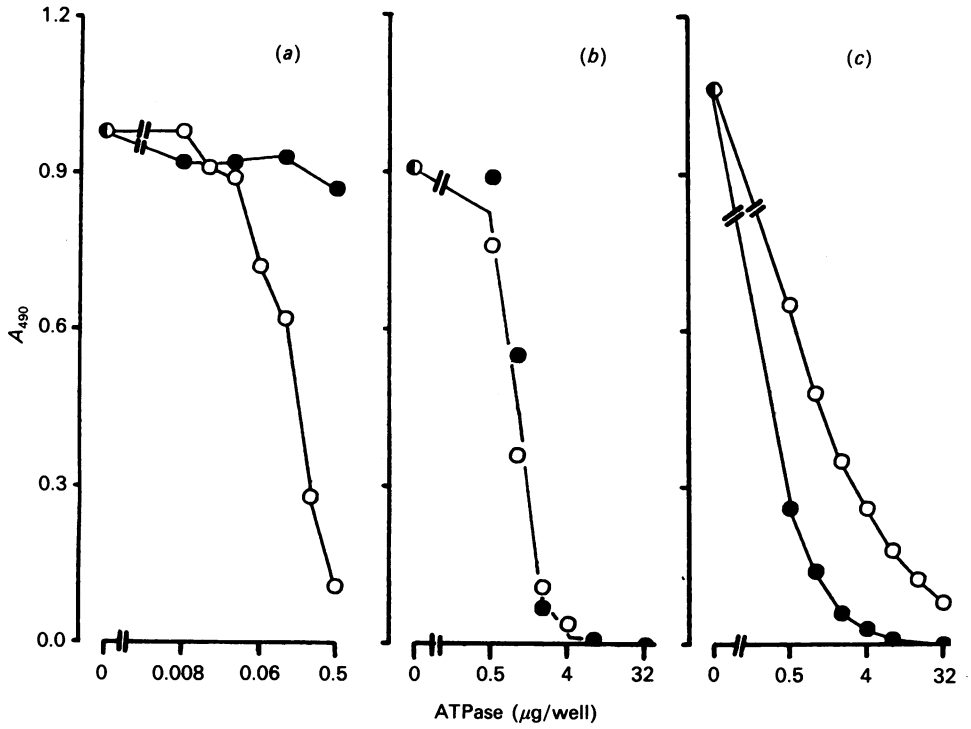

Fig. 2. Characterization of antibody binding: preference of monoclonal antibodies for native and denatured forms of $(Ca^{2+}+Mg^{2+})$-ATPase

Antibodies U^a (*a*), 4^c (*b*) and 4^a (*c*) were incubated overnight with native (○) or heat-denatured (●) ATPase at a range of concentrations. The incubate was then transferred to an e.l.i.s.a. plate coated with ATPase in order to estimate the amount of unbound antibody, which was detected by sequential incubations with horseradish-peroxidase-conjugated second antibody followed by peroxidase substrate.

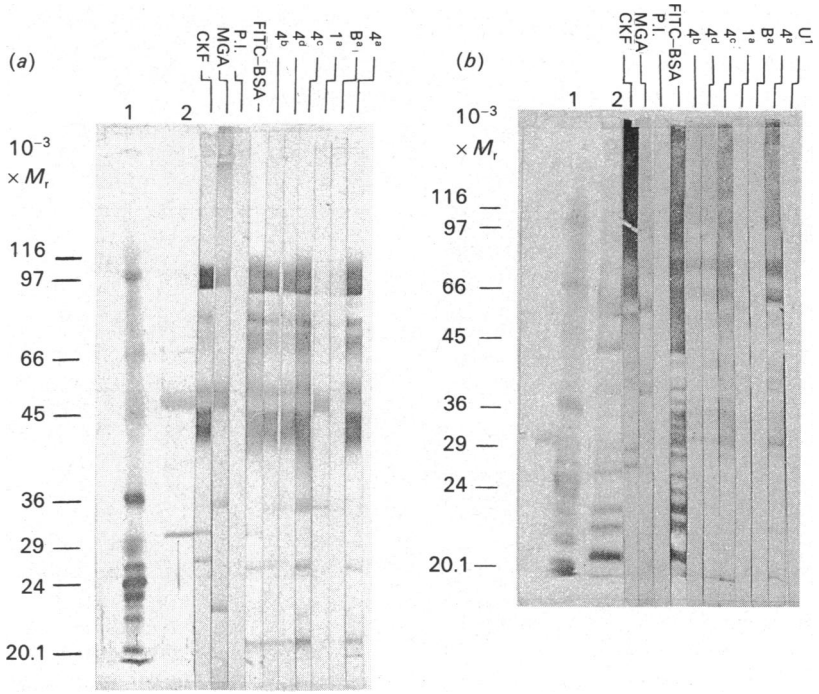

Fig. 3. Identification of epitopes on proteolytic fragments of $(Ca^{2+}+Mg^{2+})$-ATPase

(*a*) $(Ca^{2+}+Mg^{2+})$-ATPase was digested with trypsin, and the proteolysis products were resolved on polyacrylamide gels and then transferred to nitrocellulose. A portion was stained for protein with colloidal gold (lane 1, M_r standards; lane 2, digested ATPase) and the remainder was divided into strips, blocked overnight, and incubated with monoclonal antibodies (as designated), anti-*C*-terminal antibodies (CKF), anti-*N*-terminal antibodies (MGA), anti-fluorescein antibodies (FITC–BSA) or pre-immune serum (P.I.) followed by horseradish-peroxidase-conjugated second antibody, and peroxidase substrate. (*b*) $(Ca^{2+}+Mg^{2+})$-ATPase was digested with *Staphylococcus aureus* V8 protease and then treated as above.

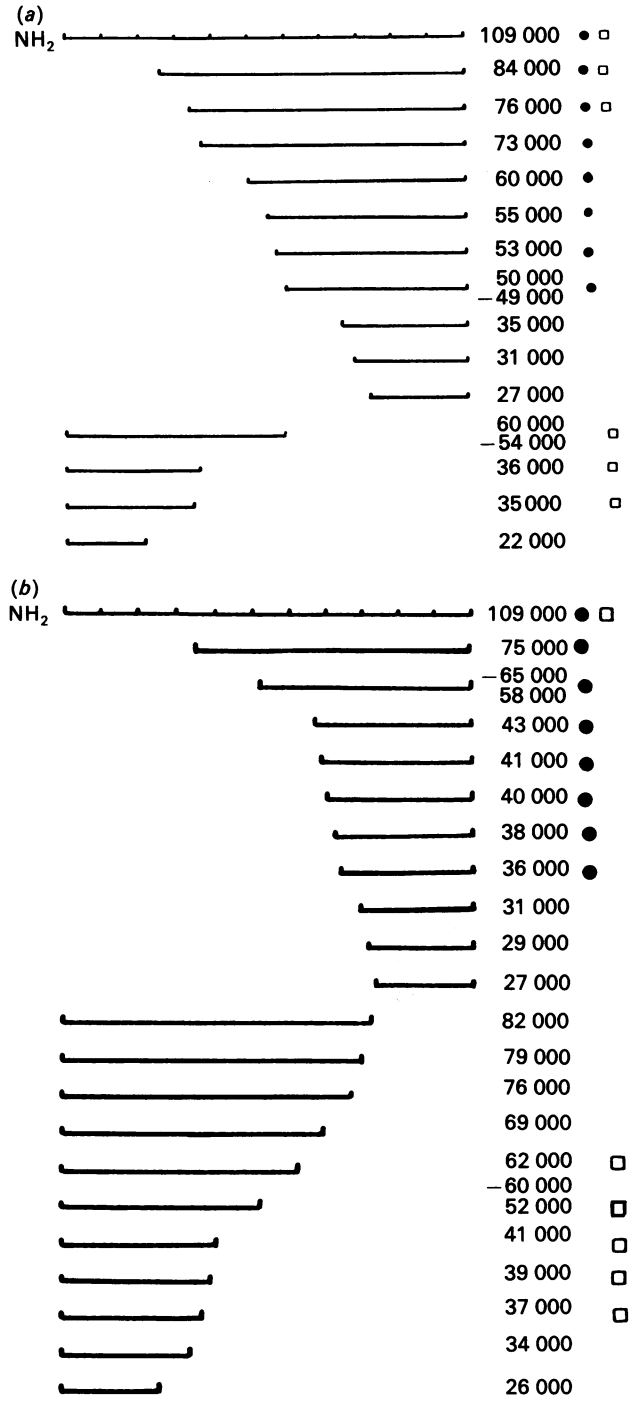

Fig. 4. Apparent M_r values of *N*- and *C*-terminal-containing fragments generated by trypsin or V8 protease digestion and their recognition by monoclonal antibodies

The apparent M_r of trypsin digest fragments seen in Fig. 3(*a*) (*a*) or the V8 protease fragments in Fig. 3(*b*) (*b*) are shown. Recognition of fragments by mAbs 4^{a-b} is denoted by ● and recognition by 1^a denoted by □.

may correspond to a *C*-terminal-containing segment since it appears to bind the anti-*C*-terminal antibody (anti-CKF). The inability of the gold stain to reveal most of the protein bands which are highlighted by the antibodies may be the result of extensive proteolysis by trypsin which would result in extremely small amounts of the larger size fragments (20000–100000) remaining. Several proteolysis products are visible by gold staining on the Western blot of the V8 protease-treated ATPase (Fig. 3*b*, lane 2), indicating that the overall digestion was less extensive.

Fig. 3(*a*) shows that mAbs 4^{a-d} recognized *C*-terminal fragments of apparent M_r-84000, -76000, -73000, -60000, -55000, -53000 and -49000–50000. These antibodies did not recognize the next smallest *C*-terminal fragment of M_r-35000 showing that they map to a region 35000–50000 from the *C*-terminus (see Fig. 4*a*). MAbs 3^{a-d} showed a similar recognition pattern and hence bind within this region (results not shown). MAb 1^a recognized the *N*-terminal-containing A fragment seen on the gold-stained digest (Fig. 3*a*, lane 2). This mAb also recognized the 36000 and 35000 *N*-terminal fragments but not the smaller fragment at 22000 (Fig. 3*a*, represented diagrammatically in Fig. 4*a*). This puts the epitope for mAb 1^a 22000–35000 from the *N*-terminus. This corresponds to an epitope on the A_1 fragment. A second group of mAbs 2^{a-d} (results not shown) were able to recognize an *N*-terminal fragment of apparent M_r 55000 (A fragment), but not the next smallest *N*-terminal fragment at 34000; hence these mAbs also map to the A_1 fragment 34000–55000 from the *N*-terminus. Using the same approach with the data for the ATPase fragments generated by V8 protease digestion (Figs. 3*b* and 4*b*), it can be demonstrated that mAbs 4^{a-d} bound within 73000–78000 of the *N*-terminus and that the epitope for mAb 1^a was positioned 34000–37000 from the *N*-terminus (represented in Fig. 4*b*). Although not shown here, mAbs 3^{a-e} were located at a region 64000–66000 from the *N*-terminus (on the B fragment) and mAbs 2^{a-d} 37000–38000 from the *N*-terminus (on the A_2 fragment). The epitope mapping data are summarized in Fig. 5. Since the V8 protease results defined the position of the epitopes most closely, these results will be used in the following discussion.

Although the accuracy of assigning M_r values is subject to an error of about 5%, the finding that the pattern of

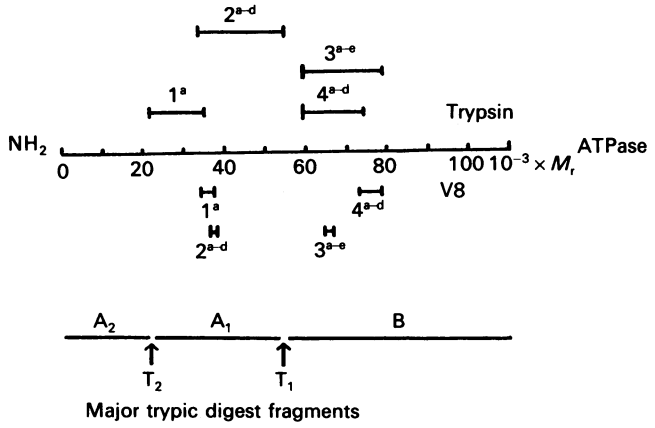

Fig. 5. Summary of epitope mapping

The epitope location of mAbs by mapping to trypsin or V8 protease digest fragments are displayed above and below the line representing the primary structure of $(Ca^{2+}+Mg^{2+})$-ATPase respectively. Also shown are the major tryptic fragments (A_1, A_2, and B) of the $(Ca^{2+}+Mg^{2+})$-ATPase and the two trypsin cleavage sites (T_1 and T_2) described by Thorley-Lawson & Green (1973).

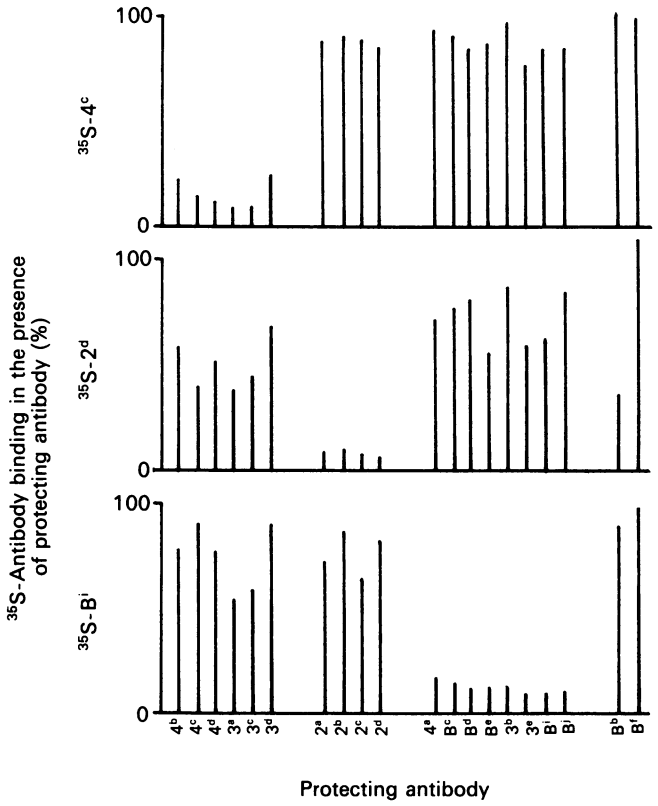

Fig. 6. Competitive binding of mAbs to (Ca^{2+} + Mg^{2+})-ATPase

E.l.i.s.a. plates coated with ATPase were incubated with excess unlabelled antibody for 3 h, after which culture medium containing ^{35}S-labelled antibodies was added to the incubation for a further 1 h. The binding of the labelled antibody was quantified by liquid scintillation counting following extensive washing of the e.l.i.s.a. plates. Binding is expressed as a percentage of the binding in the absence of competing antibody.

fragments labelled by mAbs 3^{a-d} is quite different from the pattern of fragments labelled by mAbs 4^{a-d} indicates that it is extremely unlikely that these groups of antibodies bind to the same epitope.

Fig. 6 shows the effect of competing unlabelled mAbs on the binding of ^{35}S-labelled mAbs 4^{c}, 2^{d} and B^{i} to the ATPase. These mAbs were chosen because most of the unlabelled mAbs examined could be assigned to a distinct group on the basis that they were able to inhibit binding of one of the labelled mAbs by at least 80%, but had a less marked inhibitory influence on the binding of the other two radiolabelled mAbs. The results shown are for IgG class mAbs. IgM mAbs gave irreproducible results, as did mAbs U^{a} and B^{h}, which failed to prevent the binding of labelled counterparts of themselves. Two mAbs, B^{b} and B^{f}, failed to inhibit the binding of either radiolabelled 4^{c}, 2^{d} or B^{i} and were without effect on each other's binding (results not shown), and these mAbs have been assigned to two separate groups and therefore define spatially distinct regions.

Nine mAbs significantly inhibited the steady-state ATPase activity of the (Ca^{2+} + Mg^{2+})-ATPase (Table 2). Preliminary studies showed that inhibition was complete within 60 min and that a mAb/ATPase ratio of 3:1 (mol/mol) was sufficient to effect maximal inhibition.

Table 2. Inhibition of steady state ATPase activity by mAbs

The data are expressed as percentage inhibition of control values. Control activity was typically 3.5 ± 0.2 units·mg^{-1}, measured under the conditions detailed in the Materials and methods section.

Antibody	ATPase activity (% of control)
U^{b}	52
1^{a}	43
4^{b}	64
4^{c}	68
U^{e}	39
4^{d}	44
3^{a}	39
3^{c}	56
3^{d}	60

None of the antibodies completely inhibited ATPase activity, the greatest inhibition seen being with mAb 3^{a} (61% inhibition), and none of the other 19 mAbs had any significant effect on activity (i.e. mean activity $\pm$ S.E.M. $\geqslant 90 \pm 5$%). Solubilizing concentrations of the detergent $C_{12}E_{8}$ had no significant effect on the inhibition of ATPase activity by antibody 4^{c}.

DISCUSSION

Using the available dimensional data for the (Ca^{2+} + Mg^{2+})-ATPase (Herbette *et al.*, 1985), it can be estimated that the total surface area of the ATPase is about 200 nm^2. The cross-sectional area of the F_{ab} fragment region containing the antigen-binding site is about 10 nm^2 (Amit *et al.*, 1986). Thus the surface of the ATPase would be covered by about 20 mAbs, i.e. as many as 20 spatially distinct sites, as defined by competition between mAbs for binding, may exist on the surface of the ATPase. Of course, a much larger number of non-overlapping epitopes will exist on the protein surface. In this study we have isolated 28 mAbs which bind to at least five spatially distinct sites on the ATPase as defined by the ability of mAbs to inhibit the binding of mAbs 4^{c}, 2^{d}, B^{i}, B^{b} and B^{f} (Fig. 6). Thus, with the mAbs obtained to date, we have a library which covers about 25% of the surface of the protein. The finding that many of the mAbs appear to map to a few sites on the ATPase suggests that these regions may be particularly immunogenic and accessible regions of the protein. Similar immuno-dominant regions have been demonstrated for other proteins (Atassi, 1975; Tzartos & Lindstrom, 1980).

All of the mAbs produced for this study mapped to the A_1 and B fragments of the ATPase and none were found to bind to the A_2 fragment, which is surprising because the A_2 fragment constitutes 20% of the protein. In the hypothetical structural model of Brandl *et al.* (1986), the A_2 tryptic fragment, which stretches from the *N*-terminus to the tryptic cleavage site T_2 (Figs. 5 and 7), constitutes part of the stalk region [seen in electron micrographs to connect the cytoplasmic and membrane-bound domains of the ATPase (Taylor *et al.*, 1986)] and the so-called transduction domain which is proposed to play a role in coupling ATP hydrolysis to calcium transport (Brandl

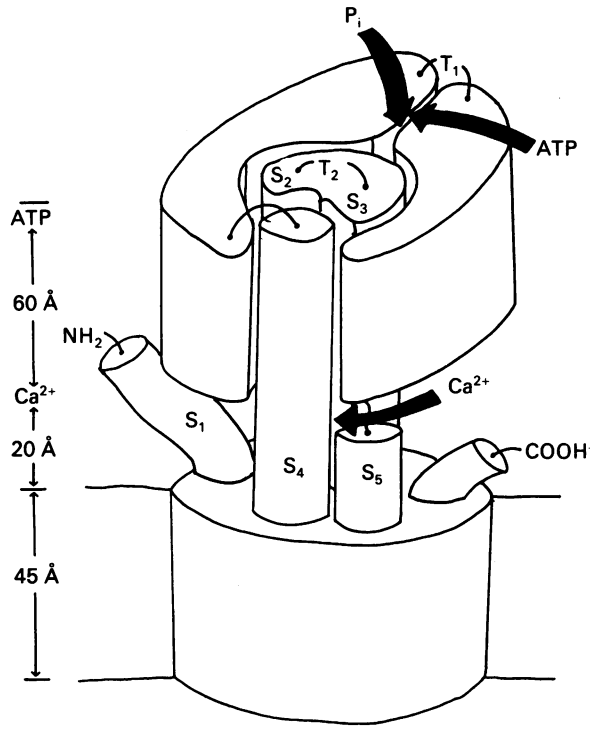

Fig. 7. Diagramatic representation of $(Ca^{2+}+Mg^{2+})$-ATPase showing the relative positions of the major domains based on the recognition of the native $(Ca^{2+}+Mg^{2+})$-ATPase by mAbs

Fragment A_2, which includes the *N*-terminus and stalk segments S_1 and S_2 (see Brandl *et al.*, 1986; also Fig. 5), is with the exception of the extreme *N*-terminus depicted as being located under and between the major domains involved in ATP hydrolysis and therefore inaccessible to antibody binding. This would explain the finding that none of the 28 mAbs recognized this fragment. The exposed regions of the ATPase in the model are S_4 and the nucleotide-binding and phosphorylation domains. The majority of mAbs in this study recognized stretches of the ATPase which in the model of Brandl *et al.* (1986) run from S_4 through the phosphorylation and nucleotide-binding domains, and as close to the *C*-terminus as the hinge region before S_5. 1 Å = 0.1 nm.

et al., 1986). The fact that no mAbs were obtained to the A_2 tryptic fragment suggests that this region of the ATPase is largely inaccessible. This has been combined with other information about the ATPase in Fig. 7. It is envisaged that although the *N*-terminal region of the protein is exposed [the antibodies produced against the *N*-terminal peptide recognized the native protein in competitive e.l.i.s.a.s (results not shown)], the part of the A_2 fragment making up the stalk region is tucked under the globular head of the protein, which comprises the phosphorylation and nucleotide-binding domains. The rest of the fragment may then lie between the nucleotide and phosphorylation domains, eventually emerging on the surface of the ATPase at the trypsin cleavage site T_2. The next epitope in the primary sequence seen in this study is that of mAb 1^a which binds 34000–37000 from the *N*-terminus (i.e. between residues 300 and 360, this includes a 5% error in estimating the M_r values from the gel, as discussed above). This indicates that the region from the T_2 trypsin site to around residue 310, which includes a further stalk helix (S_3) and two transmembranous segments M_3 and M_4 in the model of Brandl *et al.* (1986), may be unavailable for antibody binding in the native structure. To achieve such a location in the structural model, S_3 and S_2 have been assigned to positions between and beneath the nucleotide-binding and phosphorylation domains. The next stalk region, S_4, may include the epitope for mAb 1^a and it has been positioned on an outer face of the ATPase. The exposed location of the phosphorylation and nucleotide-binding domains is justified because the epitope mapping shows that a number of epitopes are located on these segments of the ATPase [i.e. mAbs 2^{a-d} which bind 37000–38000 from the *N*-terminus (this translates to residues 320–365), mAbs 3^{a-e} which bind 64000–66000 from the *N*-terminus (residues 565–635) and mAbs 4^{a-d} which bind 73000–75000 from the *N*-terminus (residues 635–720)].

The exposed nature of the nucleotide-binding and phosphorylation domains and the relative inaccessibility of the calcium-binding domain located in the stalk region [which is implicit in the model of Brandl *et al.* (1986) and substantiated by the distribution of epitopes found in this study] is also supported by fluorescence energy transfer measurements which indicate that the ATP-binding site is on the uppermost surface of the ATPase some 80 Å (8 nm) above the level of the glycerol backbone region of the lipid bilayer (Gutierrez-Merino *et al.*, 1987). The calcium-binding sites are only 20 Å (2 nm) above the glycerol backbone region (Munkonge *et al.*, 1989) which would place them in the stalk region (these data are included in Fig. 7). The clearance between the globular part of the protein and the transmembranous segments is about 16 Å (1.6 nm) (Taylor *et al.*, 1986) which would clearly prevent access of antibodies to the stalk region given that the diameter of an antigen-binding arm of an antibody is about 35 Å (3.5 nm) (Amit *et al.*, 1986).

The finding that a number of our antibodies were inhibitory (Table 2) was expected since previous studies involving mAbs against this and related ATPases have produced inhibitory mAbs (Ball *et al.*, 1986; Levitsky *et al.*, 1987). The inability of any of the inhibitory antibodies to completely inhibit activity has been reported in similar studies on the $(Na^+ + K^+)$-ATPase (Ball *et al.*, 1986). It is unlikely that this is the result of non-saturation of binding to the ATPase due to steric hindrance, since solubilizing concentrations of $C_{12}E_8$ did not increase the maximal inhibition seen with mAb 4^c.

The majority of the inhibitory mAbs (4^b, 4^c, 4^d, 3^a, 3^c and 3^d) bound to the region defined by their ability to inhibit the binding of mAb [^{35}S]4^c. Three of these mAbs (4^b, 4^c and 4^d) map to the same region (i.e. between residues 630–710). If the epitope mapping data are superimposed on to the structural model for the ATPase proposed by Brandl *et al.* (1986), it is apparent that these mAbs bind to epitopes located in the latter portion of the nucleotide-binding domain or the initial segment of the hinge region. It is this hinge domain which is thought to allow the reorientation of the nucleotide-binding domain relative to the phosphorylation domain during the catalytic cycle. The other members of these inhibitory mAbs (3^a, 3^c and 3^d) bind at epitope(s) between residues 550–640, which includes only the latter part of the nucleotide-binding domain. On the A_1 fragment, only mAb 1^a, which binds between residues 280–370 [which includes segments M_4 and S_4 and part of the phos-

phorylation domain of Brandl *et al.* (1986)] is inhibitory. The remaining inhibitory mAbs (U^b and U^c) bound exclusively to native ATPase and therefore could not be mapped. Also of importance is the finding that binding of mAbs to four out of the five spatially defined regions did not affect activity. Thus binding to the ATPase is not sufficient to cause inhibition, and presumably the epitopes to which these mAbs are bound play a relatively passive role in the events which accompany catalysis.

The mechanism(s) of the inhibition seen here is unknown but since it is known that the inhibitory antibodies which have been mapped are located on the phosphorylation and nucleotide-binding domains, it is possible that they may act either by sterically hindering the access of substrates and products to the active site or alternatively by interfering with movements which are thought to occur between these domains during the catalytic cycle (MacLennan *et al.*, 1985; Petithory & Jencks, 1986). We anticipate that these inhibitory mAbs will provide useful tools with which to examine the role of particular protein segments in the overall activity of the $(Ca^{2+} + Mg^{2+})$-ATPase as well as provide information about the spatial arrangement of epitopes on the ATPase surface.

We gratefully acknowledge the financial support of The Wellcome Trust, The Nuffield Foundation, The Smith–Kline Foundation and the Wessex Medical Trust. J.C. is a Science and Engineering Research Council Research Student and A.M.M. was funded during the course of this work by The Juan March Foundation (Spain).

REFERENCES

Amit, A. G., Marriuzza, R. A., Phillips, S. E. V. & Poljack, R. J. (1986) Science **233**, 747–753
Atassi, M. Z. (1975) Immunochemistry **2**, 423–438
Atherton, E., Logan, C. J. & Sheppard, R. C. (1981) J. Chem. Soc. Perkin Trans. 1, 538–546
Ball, W. J., Schwartz, A. & Lescard, J. L. (1986) Biochemistry **25**, 7155–7162
Brandl, C. J., Green, N. M., Korczak, B. & MacLennan, D. H. (1986) Cell **44**, 597–607
Cleveland, D. W., Fischer, S. G., Kirschner, M. W. & Laemmli, U. K. (1977) J. Biol. Chem. **252**, 1102–1106
de Meis, L. & Vianna, A. (1979) Annu. Rev. Biochem. **48**, 275–292
Dulhunty, A. F., Banyard, M. R. C. & Medveczky, C. J. (1987) J. Membr. Biol. **99**, 79–92
East, J. M. & Lee, A. G. (1982) Biochemistry **21**, 4144–4155
Ey, P. L., Prowse, S. J. & Jenkin, C. R. (1978) Immunochemistry **15**, 429–436
Froud, R. J. & Lee, R. G. (1986) Biochem. J. **237**, 197–206
Galfrè, G. & Milstein, C. (1981) Methods Enzymol. **73**, 3–46
Garcia de Ancos, J. & Inesi, G. (1988) Biochemistry **27**, 1793–1803
Gould, G. W., East, J. M., Froud, R. J., McWhirter, J. M., Stefanova, H. I. & Lee, A. G. (1986) Biochem. J. **237**, 217–227
Green, N. M., Alexander, H., Olsen, A., Alexander, S., Shinnick, T. M., Sutcliffe, J. G. & Lerner, R. A. (1982) Cell **28**, 477–487
Gutierrez-Merino, C., Munkonge, F., Mata, A. M., East, J. M., Levinson, B. L., Napier, R. M. & Lee, A. G. (1987) Biochim. Biophys. Acta **897**, 207–216
Hardwicke, P. M. D. & Green, N. M. (1974) Eur. J. Biochem. **42**, 183–193
Herbette, L., De Foor, P., Fleischer, S., Pascolini, D., Scarpa, A. & Blasie, J. K. (1985) Biochim. Biophys. Acta **817**, 103–122
Hudson, L. & Hay, F. C. (1983) Practical Immunology, 2nd edn., pp. 238–239, Blackwell, Oxford
Laemmli, U. K. (1970) Nature (London) **227**, 680–685
Levitsky, D. O., Syrbu, S. I., Cherpakhin, V. V. & Rokhlin, O. V. (1987) Eur. J. Biochem. **164**, 477–484
MacLennan, D. H., Brandl, C. J., Korczak, B. & Green, N. M. (1985) Nature (London) **316**, 696–700
Merrifield, R. B. (1986) Science **232**, 341–347
Moeremans, M., Daneels, G. & de Mey, J. (1985) Anal. Biochem. **145**, 315–321
Munkonge, F., East, J. M. & Lee, A. G. (1989) Biochim. Biophys. Acta **979**, 113–120
Petithory, J. R. & Jencks, W. P. (1986) Biochemistry **25**, 4493–4497
Schenk, D. B., Huber, J. J. & Leffert, H. L. (1984) J. Biol. Chem. **259**, 14941–14951
Shull, G. E., Schwartz, A. & Lingrel, J. B. (1985) Nature (London) **316**, 691–695
Stanker, L. H., Vanderlan, M. & Juarez-Salina, S. H. (1985) J. Immunol. Methods **76**, 157–169
Taylor, K. A., Dux, L. & Martonosi, A. (1986) J. Mol. Biol. **187**, 417–427
Thorley-Lawson, D. A. & Green, N. M. (1973) Eur. J. Biochem. **40**, 403–413
Towbin, H., Staehelin, T. & Gordon, J. (1979) Proc. Natl. Acad. Sci. U.S.A. **76**, 4350–4354
Tzartos, S. J. & Lindstrom, J. M. (1980) Proc. Natl. Acad. Sci. U.S.A. **77**, 755–759
Zubrzycka-Gaarn, E., MacDonald, G., Phillips, L., Jorgensen, A. & MacLennan, D. H. (1984) J. Bioenerg. Biomembr. **16**, 441–464

Received 5 December 1988/23 March 1989; accepted 13 April 1989